

Double-helicity dependence of jet properties from dihadrons in longitudinally polarized $p + p$ collisions at $\sqrt{s} = 200$ GeV

A. Adare,¹¹ S. Afanasiev,²⁵ C. Aidala,^{12,33,36} N. N. Ajitanand,⁵³ Y. Akiba,^{47,48} H. Al-Bataineh,⁴² J. Alexander,⁵³ K. Aoki,^{30,47} L. Aphecetche,⁵⁵ R. Armendariz,⁴² S. H. Aronson,⁶ J. Asai,^{47,48} E. C. Aschenauer,⁶ E. T. Atomssa,³¹ R. Averbek,⁵⁴ T. C. Awes,⁴³ B. Azmoun,⁶ V. Babintsev,²¹ M. Bai,⁵ G. Baksay,¹⁷ L. Baksay,¹⁷ A. Baldisseri,¹⁴ K. N. Barish,⁷ P. D. Barnes,³³ B. Bassalleck,⁴¹ A. T. Basye,¹ S. Bathe,⁷ S. Batsouli,⁴³ V. Baublis,⁴⁶ C. Baumann,³⁷ A. Bazilevsky,⁶ S. Belikov,^{6,*} R. Bennett,⁵⁴ A. Berdnikov,⁵⁰ Y. Berdnikov,⁵⁰ A. A. Bickley,¹¹ J. G. Boissevain,³³ H. Borel,¹⁴ K. Boyle,⁵⁴ M. L. Brooks,³³ H. Buesching,⁶ V. Bumazhnov,²¹ G. Bunce,^{6,48} S. Butsyk,^{33,54} C. M. Camacho,³³ S. Campbell,⁵⁴ B. S. Chang,⁶² W. C. Chang,² J.-L. Charvet,¹⁴ S. Chernichenko,²¹ J. Chiba,²⁶ C. Y. Chi,¹² M. Chiu,²² I. J. Choi,⁶² R. K. Choudhury,⁴ T. Chujo,^{58,59} P. Chung,⁵³ A. Churyan,²¹ V. Cianciolo,⁴³ Z. Citron,⁵⁴ C. R. Cleven,¹⁹ B. A. Cole,¹² M. P. Comets,⁴⁴ P. Constantin,³³ M. Csanád,¹⁶ T. Csörgő,²⁷ T. Dahms,⁵⁴ S. Dairaku,^{30,47} K. Das,¹⁸ G. David,⁶ M. B. Deaton,¹ K. Dehmelt,¹⁷ H. Delagrangé,⁵⁵ A. Denisov,²¹ D. d'Enterria,^{12,31} A. Deshpande,^{48,54} E. J. Desmond,⁶ O. Dietzsch,⁵¹ A. Dion,⁵⁴ M. Donadelli,⁵¹ O. Drapier,³¹ A. Drees,⁵⁴ K. A. Drees,⁵ A. K. Dubey,⁶¹ A. Durum,²¹ D. Dutta,⁴ V. Dzhordzhadze,⁷ Y. V. Efremenko,⁴³ J. Egdemir,⁵⁴ F. Ellinghaus,¹¹ W. S. Emam,⁷ T. Engelmöser,¹² A. Enokizono,³² H. En'yo,^{47,48} S. Esumi,⁵⁸ K. O. Eyster,⁷ B. Fadem,³⁸ D. E. Fields,^{41,48} M. Finger, Jr.,^{8,25} M. Finger,^{8,25} F. Fleuret,³¹ S. L. Fokin,²⁹ Z. Fraenkel,^{61,*} J. E. Frantz,⁵⁴ A. Franz,⁶ A. D. Frawley,¹⁸ K. Fujiwara,⁴⁷ Y. Fukao,^{30,47} T. Fusayasu,⁴⁰ S. Gadrat,³⁴ I. Garishvili,⁵⁶ A. Glenn,¹¹ H. Gong,⁵⁴ M. Gonin,³¹ J. Gosset,¹⁴ Y. Goto,^{47,48} R. Granier de Cassagnac,³¹ N. Grau,^{12,24} S. V. Greene,⁵⁹ M. Grosse Perdekamp,^{22,48} T. Gunji,¹⁰ H.-Å. Gustafsson,³⁵ T. Hachiya,²⁰ A. Hadj Henni,⁵⁵ C. Haegemann,⁴¹ J. S. Haggerty,⁶ H. Hamagaki,¹⁰ R. Han,⁴⁵ H. Harada,²⁰ E. P. Hartouni,³² K. Haruna,²⁰ E. Haslum,³⁵ R. Hayano,¹⁰ M. Heffner,³² T. K. Hemmick,⁵⁴ T. Hester,⁷ X. He,¹⁹ H. Hiejima,²² J. C. Hill,²⁴ R. Hobbs,⁴¹ M. Hohlmann,¹⁷ W. Holzmann,⁵³ K. Homma,²⁰ B. Hong,²⁸ T. Horaguchi,^{10,47,57} D. Hornback,⁵⁶ S. Huang,⁵⁹ T. Ichihara,^{47,48} R. Ichimiya,⁴⁷ H. Inuma,^{30,47} Y. Ikeda,⁵⁸ K. Imai,^{30,47} J. Imrek,¹⁵ M. Inaba,⁵⁸ Y. Inoue,^{49,47} D. Isenhower,¹ L. Isenhower,¹ M. Ishihara,⁴⁷ T. Isobe,¹⁰ M. Issah,⁵³ A. Isupov,²⁵ D. Ivanishev,⁴⁶ B. V. Jacak,^{54,†} J. Jia,¹² J. Jin,¹² O. Jinnouchi,⁴⁸ B. M. Johnson,⁶ K. S. Joo,³⁹ D. Jouan,⁴⁴ F. Kajihara,¹⁰ S. Kametani,^{10,47,60} N. Kamihara,^{47,48} J. Kamin,⁵⁴ M. Kaneta,⁴⁸ J. H. Kang,⁶² H. Kanou,^{47,57} J. Kapustinsky,³³ D. Kawall,^{36,48} A. V. Kazantsev,²⁹ T. Kempel,²⁴ A. Khanzadeev,⁴⁶ K. M. Kijima,²⁰ J. Kikuchi,⁶⁰ B. I. Kim,²⁸ D. H. Kim,³⁹ D. J. Kim,⁶² E. Kim,⁵² S. H. Kim,⁶² E. Kinney,¹¹ K. Kiriluk,¹¹ Á. Kiss,¹⁶ E. Kistenev,⁶ A. Kiyomichi,⁴⁷ J. Klay,³² C. Klein-Boesing,³⁷ L. Kochenda,⁴⁶ V. Kochetkov,²¹ B. Komkov,⁴⁶ M. Konno,⁵⁸ J. Koster,²² D. Kotchetkov,⁷ A. Kozlov,⁶¹ A. Král,¹³ A. Kravitz,¹² J. Kubart,^{8,23} G. J. Kunde,³³ N. Kurihara,¹⁰ K. Kurita,^{49,47} M. Kurosawa,⁴⁷ M. J. Kweon,²⁸ Y. Kwon,^{56,62} G. S. Kyle,⁴² R. Lacey,⁵³ Y.-S. Lai,¹² Y. S. Lai,¹² J. G. Lajoie,²⁴ D. Layton,²² A. Lebedev,²⁴ D. M. Lee,³³ K. B. Lee,²⁸ M. K. Lee,⁶² T. Lee,⁵² M. J. Leitch,³³ M. A. L. Leite,⁵¹ B. Lenzi,⁵¹ P. Liebing,⁴⁸ T. Liška,¹³ A. Litvinenko,²⁵ H. Liu,⁴² M. X. Liu,³³ X. Li,⁹ B. Love,⁵⁹ D. Lynch,⁶ C. F. Maguire,⁵⁹ Y. I. Makdisi,⁵ A. Malakhov,²⁵ M. D. Malik,⁴¹ V. I. Manko,²⁹ E. Mannel,¹² Y. Mao,^{45,47} L. Mašek,^{8,23} H. Masui,⁵⁸ F. Matathias,¹² M. McCumber,⁵⁴ P. L. McGaughey,³³ N. Means,⁵⁴ B. Meredith,²² Y. Miake,⁵⁸ P. Mikeš,^{8,23} K. Miki,⁵⁸ T. E. Miller,⁵⁹ A. Milov,^{6,54} S. Mioduszewski,⁶ M. Mishra,³ J. T. Mitchell,⁶ M. Mitrovski,⁵³ A. K. Mohanty,⁴ Y. Morino,¹⁰ A. Morreale,⁷ D. P. Morrison,⁶ T. V. Moukhanova,²⁹ D. Mukhopadhyay,⁵⁹ J. Murata,^{49,47} S. Nagamiya,²⁶ Y. Nagata,⁵⁸ J. L. Nagle,¹¹ M. Naglis,⁶¹ M. I. Nagy,¹⁶ I. Nakagawa,^{47,48} Y. Nakamiya,²⁰ T. Nakamura,²⁰ K. Nakano,^{47,57} J. Newby,³² M. Nguyen,⁵⁴ T. Niita,⁵⁸ B. E. Norman,³³ R. Nouicer,⁶ A. S. Nyanin,²⁹ E. O'Brien,⁶ S. X. Oda,¹⁰ C. A. Ogilvie,²⁴ H. Ohnishi,⁴⁷ K. Okada,⁴⁸ M. Oka,⁵⁸ O. O. Omiwade,¹ Y. Onuki,⁴⁷ A. Oskarsson,³⁵ M. Ouchida,²⁰ K. Ozawa,¹⁰ R. Pak,⁶ D. Pal,⁵⁹ A. P. T. Palounek,³³ V. Pantuev,⁵⁴ V. Papavassiliou,⁴² J. Park,⁵² W. J. Park,²⁸ S. F. Pate,⁴² H. Pei,²⁴ J.-C. Peng,²² H. Pereira,¹⁴ V. Peresedov,²⁵ D. Yu. Peressounko,²⁹ C. Pinkenburg,⁶ M. L. Purschke,⁶ A. K. Purwar,³³ H. Qu,¹⁹ J. Rak,⁴¹ A. Rakotozafindrabe,³¹ I. Ravinovich,⁶¹ K. F. Read,^{43,56} S. Rembeczki,¹⁷ M. Reuter,⁵⁴ K. Reygers,³⁷ V. Riabov,⁴⁶ Y. Riabov,⁴⁶ D. Roach,⁵⁹ G. Roche,³⁴ S. D. Rolnick,⁷ A. Romana,^{31,*} M. Rosati,²⁴ S. S. E. Rosendahl,³⁵ P. Rosnet,³⁴ P. Rukoyatkin,²⁵ P. Ružička,²³ V. L. Rykov,⁴⁷ B. Sahlmueller,³⁷ N. Saito,^{30,47,48} T. Sakaguchi,⁶ S. Sakai,⁵⁸ K. Sakashita,^{47,57} H. Sakata,²⁰ V. Samsonov,⁴⁶ S. Sato,²⁶ T. Sato,⁵⁸ S. Sawada,²⁶ K. Sedgwick,⁷ J. Seele,¹¹ R. Seidl,²² A. Yu. Semenov,²⁴ V. Semenov,²¹ R. Seto,⁷ D. Sharma,⁶¹ I. Shein,²¹ A. Shevel,^{46,53} T.-A. Shibata,^{47,57} K. Shigaki,²⁰ M. Shimomura,⁵⁸ K. Shoji,^{30,47} P. Shukla,⁴ A. Sickles,^{6,54} C. L. Silva,⁵¹ D. Silvermyr,⁴³ C. Silvestre,¹⁴ K. S. Sim,²⁸ B. K. Singh,³ C. P. Singh,³ V. Singh,³ S. Skutnik,²⁴ M. Slunečka,^{8,25} A. Soldatov,²¹ R. A. Soltz,³² W. E. Sondheim,³³ S. P. Sorensen,⁵⁶ I. V. Sourikova,⁶ F. Staley,¹⁴ P. W. Stankus,⁴³ E. Stenlund,³⁵ M. Stepanov,⁴² A. Ster,²⁷ S. P. Stoll,⁶ T. Sugitate,²⁰ C. Suire,⁴⁴ A. Sukhanov,⁶ J. Sziklai,²⁷ T. Tabaru,⁴⁸ S. Takagi,⁵⁸ E. M. Takagui,⁵¹ A. Taketani,^{47,48} R. Tanabe,⁵⁸ Y. Tanaka,⁴⁰ K. Tanida,^{47,48} M. J. Tannenbaum,⁶ A. Taranenko,⁵³ P. Tarján,¹⁵ H. Themann,⁵⁴ T. L. Thomas,⁴¹

M. Togawa,^{30,47} A. Toia,⁵⁴ J. Tojo,⁴⁷ L. Tomášek,²³ Y. Tomita,⁵⁸ H. Torii,^{20,47} R. S. Towell,¹ V.-N. Tram,³¹ I. Tserruya,⁶¹ Y. Tsuchimoto,²⁰ C. Vale,²⁴ H. Valle,⁵⁹ H. W. van Hecke,³³ A. Veicht,²² J. Velkovska,⁵⁹ R. Vértesi,¹⁵ A. A. Vinogradov,²⁹ M. Virius,¹³ V. Vrba,²³ E. Vznuzdaev,⁴⁶ M. Wagner,^{30,47} D. Walker,⁵⁴ X.R. Wang,⁴² Y. Watanabe,^{47,48} F. Wei,²⁴ J. Wessels,³⁷ S. N. White,⁶ D. Winter,¹² C. L. Woody,⁶ M. Wysocki,¹¹ W. Xie,⁴⁸ Y. L. Yamaguchi,⁶⁰ K. Yamaura,²⁰ R. Yang,²² A. Yanovich,²¹ Z. Yasin,⁷ J. Ying,¹⁹ S. Yokkaichi,^{47,48} G. R. Young,⁴³ I. Younus,⁴¹ I. E. Yushmanov,²⁹ W. A. Zajc,¹² O. Zaudtke,³⁷ C. Zhang,⁴³ S. Zhou,⁹ J. Zimányi,^{27,*} and L. Zolin²⁵

(PHENIX Collaboration)

¹Abilene Christian University, Abilene, Texas 79699, USA²Institute of Physics, Academia Sinica, Taipei 11529, Taiwan³Department of Physics, Banaras Hindu University, Varanasi 221005, India⁴Bhabha Atomic Research Centre, Bombay 400 085, India⁵Collider-Accelerator Department, Brookhaven National Laboratory, Upton, New York 11973-5000, USA⁶Physics Department, Brookhaven National Laboratory, Upton, New York 11973-5000, USA⁷University of California-Riverside, Riverside, California 92521, USA⁸Charles University, Ovocný trh 5, Praha 1, 116 36, Prague, Czech Republic⁹China Institute of Atomic Energy (CIAE), Beijing, People's Republic of China¹⁰Center for Nuclear Study, Graduate School of Science, University of Tokyo, 7-3-1 Hongo, Bunkyo, Tokyo 113-0033, Japan¹¹University of Colorado, Boulder, Colorado 80309, USA¹²Columbia University, New York, New York 10027, USA and Nevis Laboratories, Irvington, New York 10533, USA¹³Czech Technical University, Zikova 4, 166 36 Prague 6, Czech Republic¹⁴Dapnia, CEA Saclay, F-91191, Gif-sur-Yvette, France¹⁵Debrecen University, H-4010 Debrecen, Egyetem tér 1, Hungary¹⁶ELTE, Eötvös Loránd University, H-1117 Budapest, Pázmány P. s. 1/A, Hungary¹⁷Florida Institute of Technology, Melbourne, Florida 32901, USA¹⁸Florida State University, Tallahassee, Florida 32306, USA¹⁹Georgia State University, Atlanta, Georgia 30303, USA²⁰Hiroshima University, Kagamiyama, Higashi-Hiroshima 739-8526, Japan²¹IHEP Protvino, State Research Center of Russian Federation, Institute for High Energy Physics, Protvino, 142281, Russia²²University of Illinois at Urbana-Champaign, Urbana, Illinois 61801, USA²³Institute of Physics, Academy of Sciences of the Czech Republic, Na Slovance 2, 182 21 Prague 8, Czech Republic²⁴Iowa State University, Ames, Iowa 50011, USA²⁵Joint Institute for Nuclear Research, 141980 Dubna, Moscow Region, Russia²⁶KEK, High Energy Accelerator Research Organization, Tsukuba, Ibaraki 305-0801, Japan²⁷KFKI Research Institute for Particle and Nuclear Physics of the Hungarian Academy of Sciences (MTA KFKI RMKI), H-1525 Budapest 114, PO Box 49, Budapest, Hungary²⁸Korea University, Seoul, 136-701, Korea²⁹Russian Research Center "Kurchatov Institute," Moscow, Russia³⁰Kyoto University, Kyoto 606-8502, Japan³¹Laboratoire Leprince-Ringuet, Ecole Polytechnique, CNRS-IN2P3, Route de Saclay, F-91128, Palaiseau, France³²Lawrence Livermore National Laboratory, Livermore, California 94550, USA³³Los Alamos National Laboratory, Los Alamos, New Mexico 87545, USA³⁴LPC, Université Blaise Pascal, CNRS-IN2P3, Clermont-Fd, 63177 Aubiere Cedex, France³⁵Department of Physics, Lund University, Box 118, SE-221 00 Lund, Sweden³⁶Department of Physics, University of Massachusetts, Amherst, Massachusetts 01003-9337, USA³⁷Institut für Kernphysik, University of Muenster, D-48149 Muenster, Germany³⁸Muhlenberg College, Allentown, Pennsylvania 18104-5586, USA³⁹Myongji University, Yongin, Kyonggido 449-728, Korea⁴⁰Nagasaki Institute of Applied Science, Nagasaki-shi, Nagasaki 851-0193, Japan⁴¹University of New Mexico, Albuquerque, New Mexico 87131, USA⁴²New Mexico State University, Las Cruces, New Mexico 88003, USA⁴³Oak Ridge National Laboratory, Oak Ridge, Tennessee 37831, USA⁴⁴IPN-Orsay, Université Paris Sud, CNRS-IN2P3, BP1, F-91406, Orsay, France⁴⁵Peking University, Beijing, People's Republic of China⁴⁶PNPI, Petersburg Nuclear Physics Institute, Gatchina, Leningrad region, 188300, Russia⁴⁷RIKEN Nishina Center for Accelerator-Based Science, Wako, Saitama 351-0198, Japan⁴⁸RIKEN BNL Research Center, Brookhaven National Laboratory, Upton, New York 11973-5000, USA⁴⁹Physics Department, Rikkyo University, 3-34-1 Nishi-Ikebukuro, Toshima, Tokyo 171-8501, Japan

⁵⁰*Saint Petersburg State Polytechnic University, St. Petersburg, Russia*⁵¹*Universidade de São Paulo, Instituto de Física, Caixa Postal 66318, São Paulo CEP05315-970, Brazil*⁵²*System Electronics Laboratory, Seoul National University, Seoul, Korea*⁵³*Chemistry Department, Stony Brook University, SUNY, Stony Brook, New York 11794-3400, USA*⁵⁴*Department of Physics and Astronomy, Stony Brook University, SUNY, Stony Brook, New York 11794, USA*⁵⁵*SUBATECH (Ecole des Mines de Nantes, CNRS-IN2P3, Université de Nantes) BP 20722-44307, Nantes, France*⁵⁶*University of Tennessee, Knoxville, Tennessee 37996, USA*⁵⁷*Department of Physics, Tokyo Institute of Technology, Oh-okayama, Meguro, Tokyo 152-8551, Japan*⁵⁸*Institute of Physics, University of Tsukuba, Tsukuba, Ibaraki 305, Japan*⁵⁹*Vanderbilt University, Nashville, Tennessee 37235, USA*⁶⁰*Waseda University, Advanced Research Institute for Science and Engineering, 17 Kikui-cho, Shinjuku-ku, Tokyo 162-0044, Japan*⁶¹*Weizmann Institute, Rehovot 76100, Israel*⁶²*Yonsei University, IPAP, Seoul 120-749, Korea*

(Received 6 October 2009; published 15 January 2010)

It has been postulated that partonic orbital angular momentum can lead to a significant double-helicity dependence in the net transverse momentum of Drell-Yan dileptons produced in longitudinally polarized $p + p$ collisions. Analogous effects are also expected for dijet production. If confirmed by experiment, this hypothesis, which is based on semiclassical arguments, could lead to a new approach for studying the contributions of orbital angular momentum to the proton spin. We report the first measurement of the double-helicity dependence of the dijet transverse momentum in longitudinally polarized $p + p$ collisions at $\sqrt{s} = 200$ GeV from data taken by the PHENIX experiment in 2005 and 2006. The analysis deduces the transverse momentum of the dijet from the widths of the near- and far-side peaks in the azimuthal correlation of the dihadrons. When averaged over the transverse momentum of the triggered particle, the difference of the root mean square of the dijet transverse momentum between like- and unlike-helicity collisions is found to be $-37 \pm 88^{\text{stat}} \pm 14^{\text{sys}}$ MeV/c.

DOI: [10.1103/PhysRevD.81.012002](https://doi.org/10.1103/PhysRevD.81.012002)

PACS numbers: 13.75.Cs, 14.20.Dh, 21.10.Hw

I. INTRODUCTION

Since the startling 1989 result of the European Muon Collaboration, which revealed that much less of the proton spin is carried by the quark and antiquark spins than previously expected [1], there has been great interest in the angular momentum structure of the nucleon. Subsequent deep-inelastic scattering experiments have confirmed that only $\sim 20\%$ – 30% of the proton spin is due to quark and antiquark polarization [2,3].

The remainder of the spin of the proton must be due to gluon spin and/or partonic orbital angular momentum (OAM). It is known that the proton anomalous magnetic moment requires in general some orbital angular momentum of the quarks; however, this motion of the quarks does not necessarily make a net contribution to the spin of the proton (see e.g. [4,5]). Recent measurements of ΔG , the gluon spin contribution to the proton, are still statistically limited but have excluded large values of gluon polarization [6–8], and the most recent global study indicates nearly vanishing gluon polarization in the presently accessible x range, together with a small quark polarization [9]. Forthcoming data from the Relativistic Heavy Ion Collider (RHIC) should place tighter constraints on ΔG and shed new light on the spin puzzle. Meanwhile, progress in the

quark and gluon helicity distributions has served to help fuel the increasing interest in orbital angular momentum that began in the 1990s.

It is important to note that while the total spin of the proton as $\frac{1}{2}\hbar$ is well defined, there is no unique way to describe the decomposition of the angular momentum among the interacting partons within a nucleon (see e.g. [10]). Thus discussions of partonic orbital angular momentum in the proton typically involve a number of subtleties, despite the relatively intuitive nature of the concept. Two decompositions of nucleon angular momentum that have become standard are that of Jaffe and Manohar [11] and that of Ji [12]. While at present no quantitative method is known to probe experimentally the partonic OAM of the Jaffe-Manohar decomposition, in Ji's paper he proposes the experimental technique of deeply virtual Compton scattering to access quark OAM via generalized parton distributions (GPDs). Several groups have already pursued this experimentally challenging path [13–19]. Initial measurements of hard exclusive lepton production of vector mesons, another means of accessing GPDs, have also been performed [20–22]. Within the Ji decomposition, results for the OAM of up and down quarks have become available from lattice quantum chromodynamics (QCD) calculations [23]. These lattice QCD results suggest that the orbital angular momentum for u and d quarks separately is quite substantial, but that these contributions largely cancel in the proton.

*Deceased.

†PHENIX spokesperson: jacak@skipper.physics.sunysb.edu.

Another approach to studying the transverse motion of quarks and gluons within the nucleon is through transverse-momentum-dependent parton distribution functions (TMDs). The first attempt to use a TMD to describe the large transverse single-spin asymmetries observed in polarized hadronic collisions was made by Sivers in a 1990 paper [24], and the various TMDs contributing to the leading-order polarized semi-inclusive deep-inelastic scattering cross section were laid out by Mulders and Tangerman in 1996 [25]. Progress was made in both experiment and theory throughout the decade, but it was only after some key theoretical developments in 2002–2003 [26–28] that an ongoing period of intense theoretical and experimental activity regarding TMDs began. It should be noted that thus far, no model-independent quantitative relationship between TMDs and parton orbital angular momentum has been derived [29,30], and it is not clear at present if the OAM to which TMDs could provide sensitivity would fit within either the Jaffe-Manohar or Ji decomposition of nucleon angular momentum.

While the majority of work related to investigating OAM of the partons within the nucleon has taken place since the 1990s, an early theoretical discussion of orbital angular momentum inside hadrons was published by Chou and Yang in 1976 [31], describing the “hadronic matter current” inside a polarized hadron. After the EMC result [1], Meng *et al.* [32] built upon these semiclassical ideas and proposed two experiments to access rotating constituents in the nucleon, one in semi-inclusive deep-inelastic scattering of unpolarized leptons on transversely polarized protons, and the second in the measurement of the net transverse momentum of Drell-Yan pairs in collisions of longitudinally polarized protons. The latter lays the theoretical basis for this analysis: if the transverse momentum of the partons in the initial state is correlated with the (longitudinal) spin direction, then hard collisions involving these circulating partons will lead to final states with a net transverse momentum p_T with magnitude dependent upon the relative orientation of the spin directions and the impact parameter of the collision, as can be seen in Fig. 1.

For a particular helicity combination, e.g., positive on positive, the transverse momenta of the rotating partons add for peripheral collisions and give a net transverse momentum to the lepton pair (in the case of Drell-Yan). For small-impact-parameter collisions in the like-helicity combination, the helicity-correlated transverse momenta of the partons mostly cancel. In the other helicity combination (unlike sign), the opposite effect is seen, i.e., peripheral collisions give a small net transverse momentum, while small-impact-parameter collisions give a larger net transverse momentum.

The correlation of the parton transverse momentum with the orbital angular momentum is expected to depend on the spatial position of the parton in the proton. However, experimentally there is currently no technique for deter-

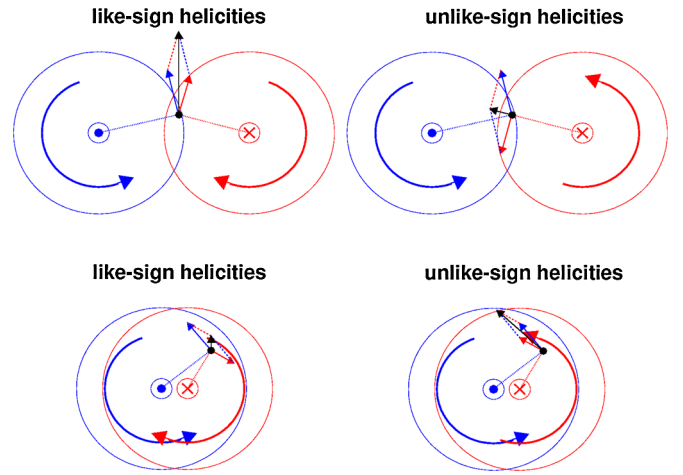


FIG. 1 (color online). Colliding protons are represented by overlapping circles, with proton momentum designated by the central symbol, and spin direction designated by the clockwise or counterclockwise arrows. A positive correlation between parton transverse momentum and proton spin has been assumed. For a like-sign helicity combination (positive on positive, left panels), the transverse momenta of the rotating partons add for peripheral collisions (top left) and result in a net transverse momentum of the lepton pair (in the case of Drell-Yan) and mostly cancel for small-impact-parameter collisions (bottom left). In the other helicity combination (unlike-sign), the opposite effect is seen, i.e., peripheral collisions lead to cancellations of the transverse momentum (top right), while small-impact-parameter collisions give a larger net transverse momentum (bottom right).

mining the impact parameter of an inelastic $p + p$ collision, and more specifically the spatial location of the parton-parton hard scattering within that geometry. Despite this limitation, in [32], with a rather simple picture of the transverse spatial distribution (homogeneous sphere) and momentum distribution (rotational momentum, k_ϕ , independent of position inside the proton), it was found that approximately half of the maximum effect ($\langle p_T^2 \rangle_{\max} = 4k_\phi^2$, when the vector transverse momenta are exactly aligned) remains after integrating over the impact parameter. This result is based on a semiclassical model, with the assumption that all interacting partons have the same rotational momentum. As in the case of TMDs, there is at present no well-defined relationship between the partonic OAM to which this method could provide sensitivity and either the Jaffe-Manohar or Ji decomposition of nucleon angular momentum. However, it is interesting to note that unlike effects due to the Sivers TMD [26], in the semiclassical model in which the current analysis is framed, the effect discussed below does not require an initial- or final-state interaction to generate a nonzero effect.

II. DRELL-YAN VS JET k_T

Here, we propose to probe the spin-correlated transverse momentum of partons within longitudinally polarized pro-

tons involved in hard collisions leading to jetlike events at the PHENIX experiment at RHIC. However, in PHENIX, due to our limited acceptance (in the central region, $\Delta\phi = \frac{\pi}{2} \times 2$ and $|\eta| < 0.35$ [33]), we do not reconstruct the true jet kinematics to access the jet transverse momentum. An alternative method has been developed [34] that examines the dihadron azimuthal angle correlation to extract the average parton transverse momentum, $\sqrt{\langle k_T^2 \rangle}$, on a statistical basis for two subsets of the data, like-helicity collisions and unlike-helicity collisions, which can then be compared as a measure of the helicity dependence of the net interacting parton transverse motion.

Since, in contrast to the Drell-Yan experiment proposed in [32], we deal here with hadronic final states, there could in principle be spin-dependent contributions to the measured $\sqrt{\langle k_T^2 \rangle}$ which are not related to the initial partonic transverse momentum. The measured dihadron transverse momentum, $\langle p_{\text{out}}^2 \rangle$, is a convolution of the measured fragmentation transverse momentum $\langle j_T^2 \rangle$ and the extracted partons' transverse momenta $\langle k_T^2 \rangle$.

With the factorization ansatz for the mean p_T^2 of the scattered partonic pair presented in [34],

$$\frac{\langle p_T^2 \rangle_{\text{pair}}}{2} = \langle k_T^2 \rangle = \langle k_T^2 \rangle^I \oplus \langle k_T^2 \rangle^S \oplus \langle k_T^2 \rangle^H, \quad (1)$$

where the superscripts I , S , and H denote intrinsic, soft (one or several soft gluons emitted), and hard (next-to-leading order) contributions, respectively, one might attempt to understand the helicity dependence of each term. The conclusion of [32] is that the difference in the intrinsic contribution to the mean square parton transverse momentum between positive- and negative-helicity protons, $\Delta\langle k_T^2 \rangle^I$, could be nonzero, since, with a net orbital angular momentum, there would be a nonzero helicity difference in the vector-summed k_T of the initial partons. $\Delta\langle k_T^2 \rangle^H$ could also be nonzero, e.g., given a helicity dependence of three-jet events. This contribution is theoretically calculable in perturbative QCD, and experimentally, contributions from a hard component should be accessible by measuring and comparing the spin-dependent k_T difference for several center-of-mass energies. As in QED [35], soft radiation in QCD is independent of the polarization of the emitting particle, so the $\langle k_T^2 \rangle^S$ term would not contribute to any spin-dependent $\langle k_T^2 \rangle$ difference.

Additionally, since $\langle j_T^2 \rangle$ is used to extract $\langle k_T^2 \rangle$ from $\langle p_{\text{out}}^2 \rangle$, it is important to note that any possible spin dependence of $\langle j_T^2 \rangle$ can be measured directly in this analysis.

The relationship of a measured $\sqrt{\langle k_T^2 \rangle}$ difference to a partonic orbital angular momentum is nontrivial. One can attempt to relate the spin-correlated parton transverse momentum to this difference:

$$\Delta\langle k_T^2 \rangle^I = \sum_{i,j} c^{ij} W^{ij} \{ \langle \vec{k}_T^i \cdot \vec{k}_T^j \rangle^{++} - \langle \vec{k}_T^i \cdot \vec{k}_T^j \rangle^{+-} \}, \quad (2)$$

where the sums are over all partons in the colliding protons, c^{ij} is the probability of an interaction of the i th and j th partons leading to the final state, W^{ij} is the (unknown) impact parameter weighting for the interaction, and \vec{k}_T^i and \vec{k}_T^j are the two-dimensional partonic transverse momenta. In the case with no spin-dependent transverse momentum (no orbital angular momentum), the difference between the $++$ (like-helicity) and the $+-$ (unlike-helicity) terms vanishes. The c^{ij} can be calculated from parton distribution functions, whereas the W^{ij} may be estimated from simulations, given a model for the impact-parameter-dependent parton distributions.

It is evident from Eq. (2) that the mixture of initial-state partons leading to a $\pi^0 - h^\pm$ final state will have an impact on the interpretation of the data. In the central arms of PHENIX, where $\pi^0 - h^\pm$ correlations are measured, PYTHIA [36] simulations show that $\sim 50\%$ of the events leading to $\pi^0 - h^\pm$ events are $g - g$ in the initial state at π^0 transverse momenta below 4 GeV/ c (from 4–7 GeV/ c the fraction is $\sim 40\%$), with $g - q$ initial states making up the majority of the remainder. Only a small fraction of the events are like-flavored $q - q$ in the initial state.

It is instructive to examine what happens if the sign of the orbital angular momentum is different for different flavors. When two partons with the same sign OAM interact in a peripheral $p + p$ collision, then the transverse momentum adds constructively as in the top left panel of Fig. 1, regardless of the sign of the OAM. However, if the two interacting partons have opposite sign OAM, then the result would be as in the right side of Fig. 1. Therefore, an equal mixture of parton interactions with like-sign OAM with unlike-sign OAM would result in a zero proton-helicity difference in the rms transverse momenta. On the other hand, if partons of a certain flavor carry no OAM, then interactions involving that flavor would contribute nothing to the effect in either helicity case, and only act as a dilution to the overall transverse momentum difference.

Given the dominance of gluon scattering for the kinematics of this measurement, then, the results could be qualitatively interpreted (within the semiclassical model presented) as due to a diluted contribution of the gluon orbital angular momentum to the partonic k_T . A more quantitative interpretation would require a model for the OAM dependence on flavor and kinematics, together with a process and experimental simulation.

III. k_T FROM DIHADRON AZIMUTHAL CORRELATIONS

In this analysis we used PHENIX high- p_T photon triggered data from RHIC runs in 2005 and 2006 at $\sqrt{s} = 200$ GeV, as has previously been published for the PHENIX π^0 cross section asymmetry (A_{LL}) analysis [6,37] with integrated luminosities of 2.5 and 6.5 pb $^{-1}$, respectively. Neutral pions were selected from photon pairs

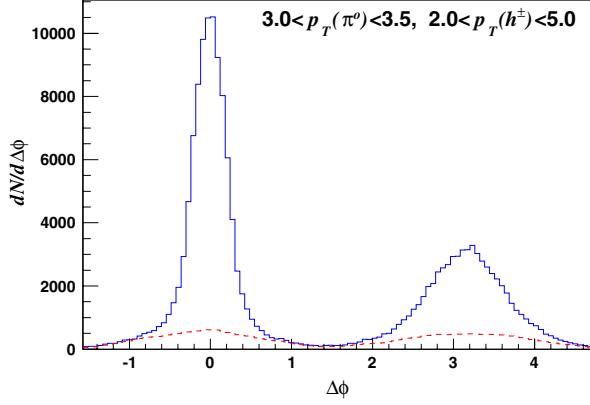


FIG. 2 (color online). Azimuthal distributions for real (solid curve) $dN_{\text{real}}/d\Delta\phi$ and mixed event (dashed curve) $dN_{\text{mix}}/d\Delta\phi$ pairs.

falling in the invariant mass region within $M_{\pi^0} \pm 2.0\sigma$. The signal-to-background ratio for the π^0 's in the range $p_T^{\pi^0} \equiv p_{Tt} > 3.0$ GeV/c is above 15.

The azimuthal correlation function is obtained by measuring the distribution of the azimuthal (around the beam axis) angle difference, $\Delta\phi = \phi_t - \phi_a$, between a π^0 (triggered particle) and a charged hadron (associated particle). The data are analyzed in eight bins of π^0 transverse momentum from 2.0 GeV/c $< p_{Tt} < 10.0$ GeV/c, and the associated charged hadron transverse momentum $p_{Ta}^{\pm} \equiv p_{Ta}$ bin is selected to be within 2.0 GeV/c $< p_{Ta} < 5.0$ GeV/c throughout this analysis. Whenever a π^0 is found in the event, the *real* ($dN_{\text{real}}/d\Delta\phi$) and *mixed* ($dN_{\text{mix}}/d\Delta\phi$) distributions are accumulated. The mixed event distribution is applied as a correction factor to account for the limited PHENIX acceptance. Mixed events are obtained by pairing a π^0 taken from a dihadron event with many charged hadrons taken from different events, randomly selected from a minimum bias data set (no high- p_T photon required) without regard to helicity. The mixed event distribution is kept the same for both helicity combinations. Figure 2 shows the real and mixed event distributions for 3.5 GeV/c $< p_{Tt}(\pi^0) < 4.5$ GeV/c.

The fragmentation transverse momentum $\sqrt{\langle j_T^2 \rangle}$ and the partonic transverse momentum $\sqrt{\langle k_T^2 \rangle}$ are related to the widths of the two peaks in the correlation function—around $\Delta\phi = 0$ degrees to obtain σ_{near} , and around $\Delta\phi = 180$ degrees to obtain $\sqrt{\langle p_{\text{out}}^2 \rangle}$ (the rms transverse momentum of the charged hadrons with respect to the π^0 's). The raw $dN_{\text{real}}/d\Delta\phi$ distribution is fit with the following function to obtain σ_{near} (based on a near-side Gaussian) and $\sqrt{\langle p_{\text{out}}^2 \rangle}$ (based on a more complicated away-side functional form, as derived in [34]):

$$\frac{dN_{\text{real}}}{d\Delta\phi} = \frac{1}{N} \frac{dN_{\text{mix}}}{d\Delta\phi} \cdot \left(C_0 + C_1 \cdot \text{Gaus}(0, \sigma_{\text{near}}) + C_2 \cdot \frac{dN_{\text{far}}}{d\Delta\phi} \Big|_{\pi/2}^{3\pi/2} \right), \quad (3)$$

where

$$\frac{dN_{\text{far}}}{d\Delta\phi} \Big|_{\pi/2}^{3\pi/2} = \frac{-p_{Ta} \cos\Delta\phi}{\sqrt{2\pi\langle p_{\text{out}}^2 \rangle} \text{Erf}(\sqrt{2}p_{Ta}/\sqrt{\langle p_{\text{out}}^2 \rangle})} \times \exp\left(-\frac{p_{Ta}^2 \sin^2\Delta\phi}{2\langle p_{\text{out}}^2 \rangle}\right). \quad (4)$$

To calculate $\sqrt{\langle j_T^2 \rangle}$ and $\sqrt{\langle k_T^2 \rangle}$ from the σ_{near} and $\sqrt{\langle p_{\text{out}}^2 \rangle}$ values obtained from the fit, the following formulas from [34] are used:

$$\sqrt{\langle j_T^2 \rangle} = \sqrt{2} \frac{p_{Tt} \cdot p_{Ta}}{\sqrt{p_{Tt}^2 + p_{Ta}^2}} \sigma_{\text{near}}, \quad (5)$$

$$\frac{\langle z_t \rangle \sqrt{\langle k_T^2 \rangle}}{\hat{x}_h} = \frac{1}{x_h} \sqrt{\langle p_{\text{out}}^2 \rangle - \langle j_{Ty}^2 \rangle (1 + x_h^2)}, \quad (6)$$

where $x_h \equiv p_{Ta}/p_{Tt}$, \hat{x}_h is the analogous ratio of the partonic transverse momenta, $\langle z_t \rangle$ is the ratio of hadronic to partonic transverse momentum for the trigger π^0 , and $\sqrt{\langle j_{Ty}^2 \rangle} = \sqrt{\langle j_T^2 \rangle}/2$.

Figure 3 and Table I show the derived values of $\langle z_t \rangle$ and \hat{x}_h , which were determined through an iterative process

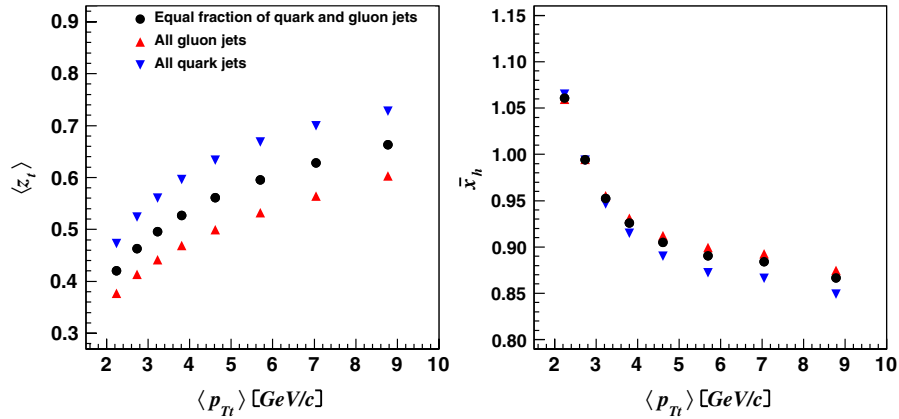


FIG. 3 (color online). Values of derived $\langle z_t \rangle$ and \hat{x}_h as explained in the text.

TABLE I. Calculated values of \hat{x}_h and $\langle z_t \rangle$ for the combined 2006 and 2005 data sets.

p_{Tt} , GeV/c	\hat{x}_h	$\langle z_t \rangle$
2.0–2.5	1.061 ± 0.003	0.42 ± 0.05
2.5–3.0	0.994 ± 0.000	0.46 ± 0.06
3.0–3.5	0.952 ± 0.004	0.50 ± 0.06
3.5–4.2	0.926 ± 0.008	0.53 ± 0.06
4.2–5.2	0.905 ± 0.011	0.56 ± 0.07
5.2–6.5	0.890 ± 0.014	0.60 ± 0.07
6.5–8.0	0.884 ± 0.013	0.63 ± 0.07
8.0–10.0	0.866 ± 0.013	0.66 ± 0.06

using a combined analysis of the measured π^0 inclusive and associated spectra using jet fragmentation functions from LEP e^+e^- measurements [38,39], as in [34]. The central values were calculated assuming an equal fraction of quark and gluon jets, while the systematic uncertainties on $\langle z_t \rangle$ and \hat{x}_h are estimated by taking the rms spread of the $g-g$, $q-q$, and equal fraction initial-state calculations.

IV. RESULTS

Fits of the $dN_{\text{real}}/d\Delta\phi$ distributions were done in three ways: (1) all data taken together (summed over the spin direction), (2) data separated into events from like-helicity and unlike-helicity collisions, and (3) the data set randomly separated into two sets of approximately equal number of events with the like-helicity and unlike-helicity collision type assigned randomly. The first is done as an update to our previously published results from 2003 data [34] with higher statistics, but with a slightly different associated charged hadron transverse momentum range, and to set the baseline for the partonic transverse momentum. The second is the measurement of interest, i.e., the difference in the net two-parton transverse momentum in like- versus unlike-helicity collisions. The results of this measurement are to be compared to the model result of [32]. The final fitting of the randomly assigned helicity combinations is done as a measure of the statistical accuracy of the fitting results, as explained below.

A. Helicity-averaged $\sqrt{\langle k_T^2 \rangle}$ and $\sqrt{\langle j_T^2 \rangle}$

The helicity-averaged fit results are enumerated in Table II for the 2006 data set. The results from the 2005 data are almost identical, with somewhat larger errors. The uncertainties on the fit parameters do not scale with statistics across the transverse momentum bins, as the uncertainty on the extraction of the width of a Gaussian distribution which is superimposed on a constant background does not scale with the statistics alone, but also depends upon the width of the Gaussian. Since the width of the peaks depends upon the p_{Tt} bin, the uncertainties do not scale with the statistics in each bin. Final statistical uncertainties on the fit parameters are determined by a statistical technique discussed below.

TABLE II. Fit parameters σ_{near} and $\sqrt{\langle p_{\text{out}}^2 \rangle}$ extracted from the helicity-averaged 2006 data set. The 2005 results are consistent within uncertainties. The uncertainties on the parameters do not scale directly with overall statistics, as discussed in the text.

p_{Tt} GeV/c	$\langle p_{Tt} \rangle$ GeV/c	$\langle p_{Ta} \rangle$ GeV/c	σ_{near}	$\sqrt{\langle p_{\text{out}}^2 \rangle}$ GeV/c
2.0–2.5	2.23	2.65	0.240 ± 0.001	1.53 ± 0.02
2.5–3.0	2.73	2.67	0.226 ± 0.001	1.42 ± 0.01
3.0–3.5	3.22	2.71	0.213 ± 0.001	1.38 ± 0.02
3.5–4.2	3.80	2.75	0.199 ± 0.001	1.28 ± 0.02
4.2–5.2	4.61	2.80	0.187 ± 0.001	1.18 ± 0.02
5.2–6.5	5.70	2.86	0.174 ± 0.002	1.09 ± 0.02
6.5–8.0	7.04	2.92	0.167 ± 0.003	1.00 ± 0.02
8.0–10.0	8.78	2.94	0.158 ± 0.004	0.96 ± 0.03

The helicity-averaged $\sqrt{\langle j_T^2 \rangle}$ and $\sqrt{\langle k_T^2 \rangle}$ results for the combined running periods are shown in Table III and in Fig. 4, where they are also compared to the previous results [34]. Note in Fig. 4 that the associated charged hadron transverse momentum bin is somewhat higher in the current analysis, but when checked by lowering the lower limit on p_{Ta} , the two results are consistent.

B. Helicity-sorted $\sqrt{\langle j_T^2 \rangle}$ and $\sqrt{\langle k_T^2 \rangle}$

The process of extracting $\sqrt{\langle j_T^2 \rangle}$ and $\sqrt{\langle k_T^2 \rangle}$ was repeated using the two subsets of the data corresponding to collisions involving like- and unlike-helicity protons at the PHENIX collision area. Since any spin-dependent effects should scale with the polarization of each beam, all helicity differences are scaled by $\frac{1}{P_B P_Y}$, where P_B and P_Y are the run-averaged beam polarizations for the two colliding beams, “blue” and “yellow,” respectively, and are $P_B = 0.50$ and $P_Y = 0.49$ in 2005, and $P_B = 0.56$ and $P_Y = 0.57$ in 2006. Uncertainties on the polarizations were propagated together for the two data sets, resulting in a 4.8% scale uncertainty in the spin-dependent differences. Uncorrelated uncertainties on the polarizations were included in the point-to-point systematic errors.

The helicity-dependent differences for $\sqrt{\langle k_T^2 \rangle}$ and $\sqrt{\langle j_T^2 \rangle}$ (averaged over the 2005 and 2006 data sets) are shown in Fig. 5. No $\sqrt{\langle j_T^2 \rangle}$ difference is observed in any p_{Tt} bin, and if we assume no p_{Tt} dependence and take the average over the p_{Tt} bins, then the average value of the difference in the fragmentation transverse momentum is $\Delta\sqrt{\langle j_T^2 \rangle} = -3 \pm 8^{\text{stat}} \pm 5^{\text{sys}}$ MeV/c, consistent with zero.

As discussed earlier, there is no quantitative expectation in the difference in $\Delta\sqrt{\langle k_T^2 \rangle}$, but any nonzero measurement can be attributed to a convolution of initial and hard scattering effects. Since no p_{Tt} dependence is expected in the model, and the data are consistent with a flat distri-

TABLE III. Combined (2005 and 2006) results for $\sqrt{\langle j_T^2 \rangle}$, $\sqrt{\langle k_T^2 \rangle}$ and the helicity-sorted differences. First errors are statistical, second are systematic. Statistical and systematic errors are determined as described in the text. Note that the majority of the systematic uncertainties are correlated and so cancel in the differences.

p_{Tl} GeV/c	No. of pairs	$\sqrt{\langle j_T^2 \rangle}$ GeV/c	$\sqrt{\langle k_T^2 \rangle}$ GeV/c	$\Delta\sqrt{\langle j_T^2 \rangle}$ GeV/c	$\Delta\sqrt{\langle k_T^2 \rangle}$ GeV/c
2.0–2.5	792 579	$0.582 \pm 0.001 \pm 0.001$	$2.96 \pm 0.03 \pm 0.36$	$-0.008 \pm 0.011 \pm 0.015$	$-0.22 \pm 0.19 \pm 0.05$
2.5–3.0	479 497	$0.613 \pm 0.002 \pm 0.001$	$2.83 \pm 0.03 \pm 0.40$	$-0.009 \pm 0.013 \pm 0.015$	$-0.11 \pm 0.19 \pm 0.03$
3.0–3.5	263 174	$0.624 \pm 0.002 \pm 0.002$	$2.87 \pm 0.03 \pm 0.38$	$0.007 \pm 0.016 \pm 0.015$	$-0.17 \pm 0.22 \pm 0.04$
3.5–4.2	180 554	$0.626 \pm 0.003 \pm 0.004$	$2.79 \pm 0.03 \pm 0.36$	$0.000 \pm 0.019 \pm 0.015$	$0.32 \pm 0.22 \pm 0.05$
4.2–5.2	101 313	$0.630 \pm 0.003 \pm 0.006$	$2.80 \pm 0.04 \pm 0.35$	$-0.014 \pm 0.023 \pm 0.015$	$0.22 \pm 0.24 \pm 0.04$
5.2–6.7	41 827	$0.634 \pm 0.005 \pm 0.009$	$2.91 \pm 0.05 \pm 0.34$	$-0.005 \pm 0.034 \pm 0.015$	$-0.03 \pm 0.33 \pm 0.02$
6.7–8.0	17 916	$0.639 \pm 0.008 \pm 0.005$	$3.01 \pm 0.07 \pm 0.39$	$0.049 \pm 0.053 \pm 0.015$	$-0.36 \pm 0.45 \pm 0.04$
8.0–10.0	6 775	$0.634 \pm 0.012 \pm 0.004$	$3.18 \pm 0.11 \pm 0.31$	$-0.024 \pm 0.082 \pm 0.015$	$-0.48 \pm 0.75 \pm 0.05$

bution, the difference is averaged over p_{Tl} to get $\Delta\sqrt{\langle k_T^2 \rangle} = -37 \pm 88^{\text{stat}} \pm 14^{\text{syst}}$ MeV/c, consistent with zero.

C. Discussion of uncertainties

To check for possible systematic errors due to spin-related beam properties or efficiencies, the beam polarization signs were randomly chosen for each event with an equal probability, the $\Delta\phi$ distributions were obtained for the two false-helicity combinations, and the fit parameters extracted. This process was repeated many times, giving distributions of the fit parameters that were well fitted with normal distributions. The widths of the fit-parameter distributions for the two false-helicity combinations are then

related to the statistical fluctuations of the fit parameters. Comparison of these widths with the errors returned from the fit indicated that the errors on the fit parameters were too small by a maximum of $\sim 15\%$, especially for p_{out} at the larger p_{Tl} bins.

In order to investigate this nonstatistical nature of the fit-parameter errors, a Monte Carlo simulation was employed. Randomly created distributions based on the shapes of the real data azimuthal distributions as a function of p_{Tl} were fitted, extracting the fit parameters and errors. This could then be repeated many times, after which the widths of the normal distributions of the extracted fit parameters were compared to the fit errors. The exact same trend as a

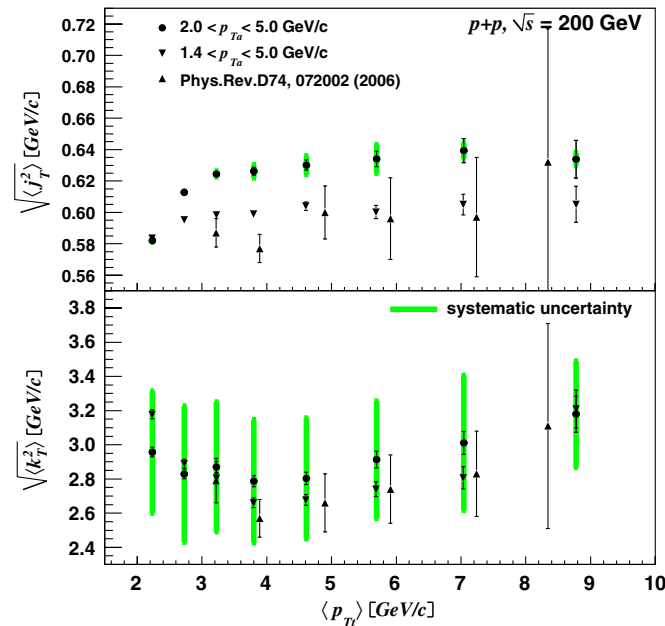


FIG. 4 (color online). Helicity-averaged $\sqrt{\langle j_T^2 \rangle}$ and $\sqrt{\langle k_T^2 \rangle}$ for combined 2005 and 2006 data. The systematic uncertainties on the $\sqrt{\langle k_T^2 \rangle}$ (green bars) are due mainly to the systematic uncertainties on the $\langle z_t \rangle$ and \hat{x}_h extractions discussed in the text.

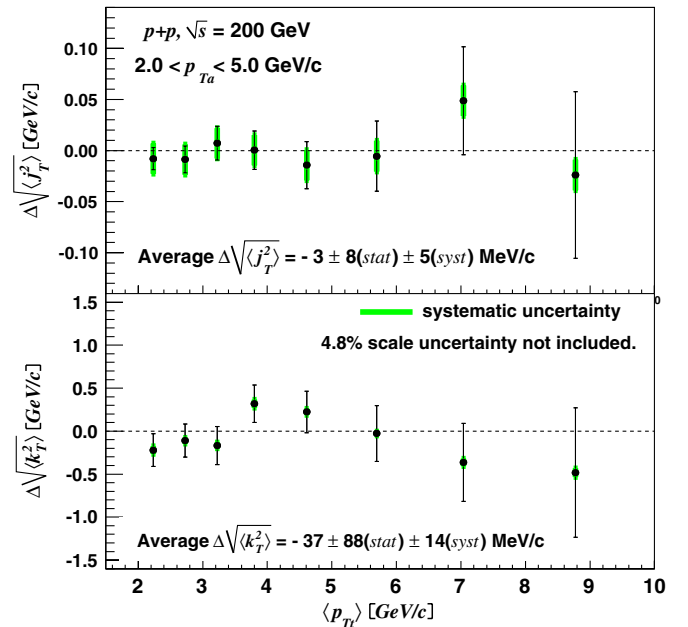


FIG. 5 (color online). Difference in $\sqrt{\langle j_T^2 \rangle}$ (top panel) and $\sqrt{\langle k_T^2 \rangle}$ (bottom panel) for like- minus unlike-helicity combinations. A systematic uncertainty of 4.8% on the vertical scale due to uncertainty in the beam polarizations is not shown. However, this uncertainty only affects the relative vertical scale.

function of p_{Tl} was seen in the Monte Carlo—the fit-parameter errors were underestimated at the larger values of p_{Tl} by $\sim 15\%$. Since the Monte Carlo is purely statistical, these results reflect the true measure of the statistical uncertainty of the fit parameters. The statistical uncertainties presented for the data are thus those obtained from the spin-randomization procedure described above.

The dominant systematic uncertainties in $\sqrt{\langle k_T^2 \rangle}$ are the uncertainties in \hat{x}_h and $\langle z_l \rangle$. Additional systematic uncertainties in $\sqrt{\langle j_T^2 \rangle}$ and $\sqrt{\langle k_T^2 \rangle}$ were determined from an analysis where the near- and away-side peaks were fit separately to determine the fit parameters. This is the dominant systematic uncertainty on $\sqrt{\langle j_T^2 \rangle}$. For $\sqrt{\langle k_T^2 \rangle}$, this was added in quadrature to the errors from \hat{x}_h and $\langle z_l \rangle$.

V. DISCUSSION

The smallness of $\Delta\sqrt{\langle j_T^2 \rangle}$ confirms the expectation that transverse momentum effects in the fragmentation should not be large in processes with a longitudinally polarized initial state and thus simplifies the interpretation of $\Delta\sqrt{\langle k_T^2 \rangle}$.

Comparing our measured value of $\Delta\sqrt{\langle k_T^2 \rangle}$ to the calculation of [32],

$$\Delta\langle p_T^2 \rangle \approx 1.9\langle k_\phi \rangle^2 \quad (7)$$

yields

$$\langle k_\phi \rangle \approx \Delta\sqrt{\langle k_T^2 \rangle} = -37 \pm 88^{\text{stat}} \pm 14^{\text{syst}} \text{ MeV}/c, \quad (8)$$

approximately an order of magnitude less than the parton intrinsic transverse momentum associated with the uncertainty limit. Assuming all contributions to this difference come from intrinsic parton motion, and taken together with the expected level of contribution from the $g-g$ channel and our model assumptions, this could qualitatively suggest a small gluon orbital angular momentum in a longitudinally polarized proton, integrated over our kinematic region. Given the modest energy scales of our measurement, of the order of a few GeV, this finding is not inconsistent with the qualitative expectation of a gluon OAM (in the Jaffe-Manohar decomposition) increasing in magnitude as a consequence of DGLAP evolution [40–43] in perturbative QCD. It is also interesting to note that the best-fit value for ΔG in the most recent global study [9] evolves quite slowly with the energy scale, leading in turn to a slow evolution in gluon OAM. A more direct connection between the present measurement and partonic OAM is complicated by the subprocess contributions and unknown impact parameter and transverse position space

weighting of the partons. In addition, further theoretical work is needed to place the model of [32] within a rigorous QCD framework. We hope that the measurement presented here will serve to encourage the theory community to pursue this task.

As discussed in Sec. I, since the 1990s there has been intense interest in partonic OAM, or more generally, in the noncollinear motion of partons within the nucleon, and there are several approaches currently being used to attempt to increase our understanding of the role that this partonic motion plays in nucleon structure, not all of which can be directly related to one another. The measurement presented here, inspired by the proposal in [32] for Drell-Yan production in longitudinally polarized $p+p$ collisions, but utilizing a dihadron correlation technique, represents a novel experimental approach to probing partonic OAM.

A dijet correlation technique in single-*transversely* polarized $p+p$ collisions has already been used at RHIC to probe the Sivers TMD [44], following a proposal in [45]. The current measurement has the potential to probe partonic OAM in a longitudinally rather than transversely polarized proton. Dijet and dihadron correlation measurements in (polarized) $p+p$ collisions provide an important tool to investigate the noncollinear motion of partons within the (polarized) nucleon, and ideas for expanding on the existing techniques would be most welcome.

VI. SUMMARY

In conclusion, $\sqrt{\langle j_T^2 \rangle}$ and $\sqrt{\langle k_T^2 \rangle}$ have been extracted from dihadron azimuthal angular correlations in longitudinally polarized $p+p$ collisions at $\sqrt{s} = 200$ GeV. The helicity differences for both quantities are consistent with zero when averaged over the π^0 transverse momentum range accessible, with a magnitude less than 5% of the corresponding spin-averaged quantities. Comparison to a similar measurement that can be performed on longitudinally polarized $p+p$ collisions at $\sqrt{s} = 500$ GeV is expected to provide additional information regarding hard vs intrinsic contributions to the measured $\Delta\sqrt{\langle k_T^2 \rangle}$. The PHENIX Collaboration collected such a data set in early 2009. Future data at RHIC will increase the statistical significance, and upcoming PHENIX upgrades will allow measurements in different kinematic regimes, changing the partonic mix probed. In the longer-term future, the accumulation of large luminosities for polarized $p+p$ collisions at RHIC should also make possible a Drell-Yan measurement, as originally proposed in [32].

ACKNOWLEDGMENTS

We thank the staff of the Collider-Accelerator and Physics Departments at Brookhaven National Laboratory and the staff of the other PHENIX participating institutions

for their vital contributions. We also thank D. Sivers, W. Vogelsang, and A. Bacchetta for helpful discussions. We acknowledge support from the Office of Nuclear Physics in the Office of Science of the Department of Energy, the National Science Foundation, a sponsored research grant from Renaissance Technologies LLC, Abilene Christian University Research Council, Research Foundation of SUNY, and Dean of the College of Arts and Sciences, Vanderbilt University (USA), Ministry of Education, Culture, Sports, Science, and Technology and the Japan Society for the Promotion of Science (Japan), Conselho Nacional de Desenvolvimento Científico e Tecnológico and Fundação de Amparo à Pesquisa do Estado de São Paulo (Brazil), Natural Science Foundation of China (People's Republic of China), Ministry of Education, Youth and Sports (Czech Republic), Centre National de la Recherche Scientifique, Commissariat à l'Énergie

Atomique, and Institut National de Physique Nucléaire et de Physique des Particules (France), Ministry of Industry, Science and Technologies, Bundesministerium für Bildung und Forschung, Deutscher Akademischer Austausch Dienst, and Alexander von Humboldt Stiftung (Germany), Hungarian National Science Fund, OTKA (Hungary), Department of Atomic Energy (India), Israel Science Foundation (Israel), Korea Research Foundation and Korea Science and Engineering Foundation (Korea), Ministry of Education and Science, Russia Academy of Sciences, Federal Agency of Atomic Energy (Russia), VR and the Wallenberg Foundation (Sweden), the U.S. Civilian Research and Development Foundation for the Independent States of the Former Soviet Union, the US-Hungarian Fulbright Foundation for Educational Exchange, and the US-Israel Binational Science Foundation.

-
- [1] J. Ashman *et al.* (European Muon Collaboration), Nucl. Phys. **B328**, 1 (1989).
- [2] A. Airapetian *et al.* (HERMES Collaboration), Phys. Rev. D **75**, 012007 (2007).
- [3] V. Y. Alexakhin *et al.* (COMPASS Collaboration), Phys. Lett. B **647**, 8 (2007).
- [4] M. Burkardt and G. Schnell, Phys. Rev. D **74**, 013002 (2006).
- [5] H. Avakian, S. J. Brodsky, A. Deur, and F. Yuan, Phys. Rev. Lett. **99**, 082001 (2007).
- [6] A. Adare *et al.* (PHENIX Collaboration), Phys. Rev. D **76**, 051106 (2007).
- [7] B. I. Abelev *et al.* (STAR Collaboration), Phys. Rev. Lett. **100**, 232003 (2008).
- [8] A. Adare *et al.* (PHENIX Collaboration), Phys. Rev. Lett. **103**, 012003 (2009).
- [9] D. de Florian, R. Sassot, M. Stratmann, and W. Vogelsang, Phys. Rev. D **80**, 034030 (2009).
- [10] M. Burkardt and H. BC, Phys. Rev. D **79**, 071501 (2009).
- [11] R. L. Jaffe and A. Manohar, Nucl. Phys. **B337**, 509 (1990).
- [12] X.-D. Ji, Phys. Rev. D **55**, 7114 (1997).
- [13] C. Munoz Camacho *et al.* (Jefferson Lab Hall A Collaboration), Phys. Rev. Lett. **97**, 262002 (2006).
- [14] A. Airapetian *et al.* (HERMES Collaboration), Phys. Rev. D **75**, 011103 (2007).
- [15] M. Mazouz *et al.* (Jefferson Lab Hall A Collaboration), Phys. Rev. Lett. **99**, 242501 (2007).
- [16] F. X. Girod *et al.* (CLAS Collaboration), Phys. Rev. Lett. **100**, 162002 (2008).
- [17] F. D. Aaron *et al.* (H1 Collaboration), Phys. Lett. B **659**, 796 (2008).
- [18] S. Chekanov *et al.* (ZEUS Collaboration), J. High Energy Phys. 05 (2009) 108.
- [19] A. Airapetian *et al.* (HERMES Collaboration), J. High Energy Phys. 06 (2008) 066.
- [20] S. Chekanov *et al.* (ZEUS Collaboration), PMC Phys. A **1**, 6 (2007).
- [21] S. A. Morrow *et al.* (CLAS Collaboration), Eur. Phys. J. A **39**, 5 (2009).
- [22] A. Airapetian *et al.* (HERMES Collaboration), Phys. Lett. B **679**, 100 (2009).
- [23] P. Hägler *et al.* (LHPC Collaboration), Phys. Rev. D **77**, 094502 (2008).
- [24] D. W. Sivers, Phys. Rev. D **41**, 83 (1990).
- [25] P. J. Mulders and R. D. Tangerman, Nucl. Phys. **B461**, 197 (1996).
- [26] S. J. Brodsky, D. S. Hwang, and I. Schmidt, Phys. Lett. B **530**, 99 (2002).
- [27] J. C. Collins, Phys. Lett. B **536**, 43 (2002).
- [28] A. V. Belitsky, X. Ji, and F. Yuan, Nucl. Phys. **B656**, 165 (2003).
- [29] S. Meissner, A. Metz, and K. Goeke, Phys. Rev. D **76**, 034002 (2007).
- [30] M. Burkardt, arXiv:0907.0296.
- [31] T. T. Chou and C. N. Yang, Nucl. Phys. **B107**, 1 (1976).
- [32] Ta-chung Meng, Ji-cai Pan, Qu-bing Xie, and Wei Zhu, Phys. Rev. D **40**, 769 (1989).
- [33] K. Adcox *et al.* (PHENIX Collaboration), Nucl. Instrum. Methods Phys. Res., Sect. A **499**, 469 (2003).
- [34] S. S. Adler *et al.* (PHENIX Collaboration), Phys. Rev. D **74**, 072002 (2006).
- [35] D. R. Yennie, S. C. Frautschi, and H. Suura, Ann. Phys. (Leipzig) **13**, 379 (1961).
- [36] T. Sjöstrand, S. Mrenna, and P. Skands, J. High Energy Phys. 05 (2006) 026.
- [37] S. S. Adler *et al.* (PHENIX Collaboration), Phys. Rev. D **73**, 091102 (2006).
- [38] P. Abreu *et al.* (DELPHI Collaboration), Eur. Phys. J. C **13**, 573 (2000).
- [39] G. Alexander *et al.* (OPAL Collaboration), Z. Phys. C **69**, 543 (1996).
- [40] V. N. Gribov and L. N. Lipatov, Sov. J. Nucl. Phys. **15**, 438

- (1972).
- [41] L.N. Lipatov, Sov. J. Nucl. Phys. **20**, 94 (1975).
- [42] Y.L. Dokshitzer, Sov. Phys. JETP **46**, 641 (1977).
- [43] G. Altarelli and G. Parisi, Nucl. Phys. **B126**, 298 (1977).
- [44] B.I. Abelev *et al.* (STAR Collaboration), Phys. Rev. Lett. **99**, 142003 (2007).
- [45] D. Boer and W. Vogelsang, Phys. Rev. D **69**, 094025 (2004).